Supplementary Information (SI) for Journal of Materials Chemistry C.

Supporting Information

Design, Synthesis, and Optoelectronic Properties of Benzothiadiazole-fused Sulfur and Nitrogen-containing Polycyclic Heteroaromatics

Yuxin Yin,[1#] Rui Shi,[2#] Zhongwei Liu,[1] Yanru Li,[1] Ting Jiang,[2] Lingxu Zhao,[2] Jie Li,[2*] Deyang Ji,[2] Liqiang Li[2] and Zhuping Fei[1, 3*]

[1)] Institute of Molecular Plus, Department of Chemistry, Key Laboratory of Organic Integrated Circuits, Ministry of Education &Tianjin Key Laboratory of Molecular Optoelectronic Science, Tianjin University, Tianjin 300072, China

[2)] Key Laboratory of Organic Integrated Circuits, Ministry of Education & Tianjin Key Laboratory of Molecular Optoelectronic Sciences, Department of Chemistry, Institute of Molecular Aggregation Science, Tianjin University, Tianjin 300072, China;

[3)] Haihe Laboratory of Sustainable Chemical Transformations, Tianjin 300192, China;

[#]These authors contributed equally.

Contents

1. Instruments and methods

2. Synthesis

3. Theoretical Calculations

4. Physiochemical characteristics

5. Organic Field-Effect Transistors Characteristics

6. Thin film morphology analysis

7. Organic Phototransistors Characteristics

8. NMR and MS (MALDI-TOF) spectrum

9. Notes and references

1. Instruments and methods

Organic Field Effect Transistor (OFET) device:

(1) OFETs device prepared by vacuum deposition (VD): The device structures are all bottom gate top contact (BGTC), i.e. Si/SiO_2/OSCs/Au or Si/SiO_2/OTS/OSCs/Au. Si/SiO_2 with a thickness of 300 nm was used for the substrate, and the cleaning process was as follows: the substrate was cleaned by ultrasonic cleaning with deionized water, acetone and isopropanol for two times, and then it was blown dry with nitrogen and put into the oven, and then it was heated by vacuum at 120 °C for 10 min, and then it was cooled down to room temperature. Organic semiconductor layers were deposited on unheated substrates or substrate surfaces at 60 °C, 80 °C, 100 °C, and 140 °C by a vapor deposition rate of 0.04 Å s^{-1}, and then 20 nm of gold was vapor-deposited as the source-drain electrodes on the surface of the organic semiconductor layers at a rate of 0.08 Å s^{-1}, and the conductive channel lengths and widths were 25 *μ*m and 200 *μ*m, respectively.

(2) Micro-nanocrystalline device prepared by physical vapor transport (PVT): Single crystals of micrometer size were slowly grown in a horizontal tube furnace by slowly introducing high-purity nitrogen, placing a quartz boat with sample powder in the high-temperature zone, and placing an OTS-treated SiO2/Si substrate in the relatively low-temperature zone. Micro/nano-sized bottom-gate-top-contact single-crystal devices have been prepared by transferring a gold film onto high-quality single-crystal as a source-drain electrode using "leaf gilding method".

Nuclear Magnetic Resonance (NMR): Both ^{1}H NMR and ^{13}C NMR tests were performed on JNM-ECZ400R (400 MHz) or JNM-ECZ600R (600 MHz) NMR spectrometer. The solvents were $CDCl_3$ or 1,1,2,2-$C_2D_2Cl_4$, and tetramethylsilane (TMS) was used as an internal standard.

Thermo Gravimetric Analysis (TGA): Tests were completed by TG 209F3 with nitrogen atmosphere and a ramp rate of 10 °C/min, with test temperatures ranging

from room temperature to 700 °C.

Differential Scanning Calorimetry (DSC): It was tested by DSC214 Polyma thermal analyzer in nitrogen atmosphere with a heating or cooling rate of 10 °C/min.

Density Functional Theory (DFT): All electronic structure calculation were performed using Gaussian 16 [1] software package. The geometric structure of investigated molecules was optimized on ground (S_0) at B3LYP-D3(BJ)/6-31G** level while no imaginary frequency was found during frequency analysis. The natural transition orbitals (NTOs) and hole-electron distribution analysis were performed by using Multiwfn program [2] to investigate corresponding excited states. The NTOs distribution were rendered by using the VMD 1.9.3 program. [3] The CT/LE percentage and supplementary parameters were obtained from hole-electron distribution analysis [4] for quantitatively evaluating the CT and LE mixing in HLCT states.

UV-Visible Spectroscopy (UV-Vis): The solution and film were tested by Shimadzu UV2600 UV spectrometer. The solvent was chloroform and the film samples were prepared from quartz sheets by vacuum evaporation at about 20 nm.

Photoluminescence (PL): The solution and film were tested by steady-state fluorescence spectrometer (FLS1000). The solvent was chloroform and the film samples were quartz sheets prepared by vacuum evaporation of about 20 nm.

Fluorescence Quantum Efficiency (PLQY): The solution and film fluorescence quantum efficiencies were tested by steady-state fluorescence spectrometer (FLS1000). The solvent was chloroform and the film samples were prepared from quartz wafers by vacuum evaporation at about 20 nm.

Ultraviolet Photoelectron Spectroscopy (UPS): The vapor-deposited film samples were measured by an instrument model AXIS ULTRA DLD using an un-

monochromatized UV source of He I. The energy of the He I light source used was 21.22 eV.

Organic Field Effect Transistor (OFET) Device Performance Testing: OFETs devices were tested on an Aglient B1500A instrument in a room temperature air environment. The carrier saturation mobility is calculated as:

$$I_{DS} = \left(\frac{W}{2L}\right) C_i \mu (V_G - V_T)^2$$

The surface trap density (N_{trap}) of bare Si/SiO2 or OTS modified Si/SiO2 is calculated as:

$$N_{trap} = \frac{C_i}{e}\left(\frac{e(SS)}{\ln 10 K_B T} - 1\right)$$

e: the fundamental unit charge; SS: the subthreshold swing; KB: the Boltzmann constant; T: the temperature.

Organic Phototransistor (OPT) Device Performance Testing: Light source instrument model is HSX-UV300 and tested in room temperature air environment. Photosensitivity (P), photoresponsivity (R) and specific detection rate (D*) were calculated as:

$$P = (I_{light} - I_{dark})/I_{dark}$$

$$R = (I_{light} - I_{dark})/(SP_{in})$$

$$D^* = RS^{1/2}(2eI_{dark})^{-1/2}$$

X-Ray Diffraction (XRD): Both in-plane and out-of-plane XRD of semiconductor films were tested on MiniFlex600 instrument in a room temperature air environment.

Atomic Force Microscopy (AFM): The film microforms, film thickness and surface roughness were determined on Bruker Dimension Icon atomic force microscope in knockdown mode.

2. Synthesis

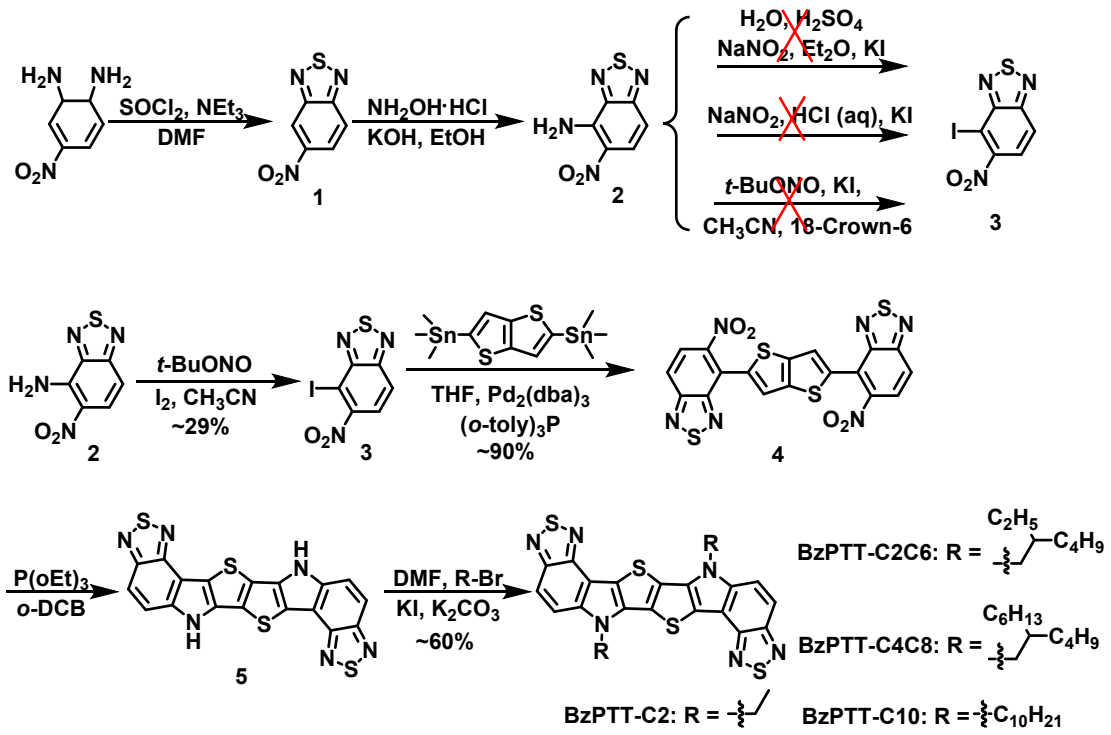

Scheme S1 The synthetic route to BzPTT-C2, BzPTT-C2C6, BzPTT-C4C8, BzPTT-C10.

3. Theoretical Calculations

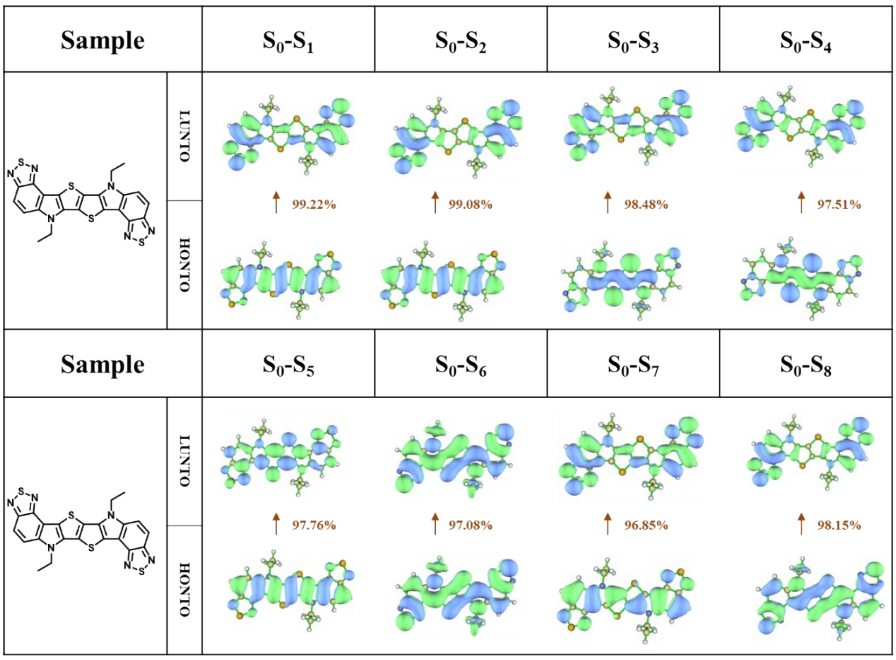

Fig.S1 HONTO and LUNTO orbital jumps of BzPTT-C2, calculated by NTO(TDDFT-B3LYP/6-31G**)

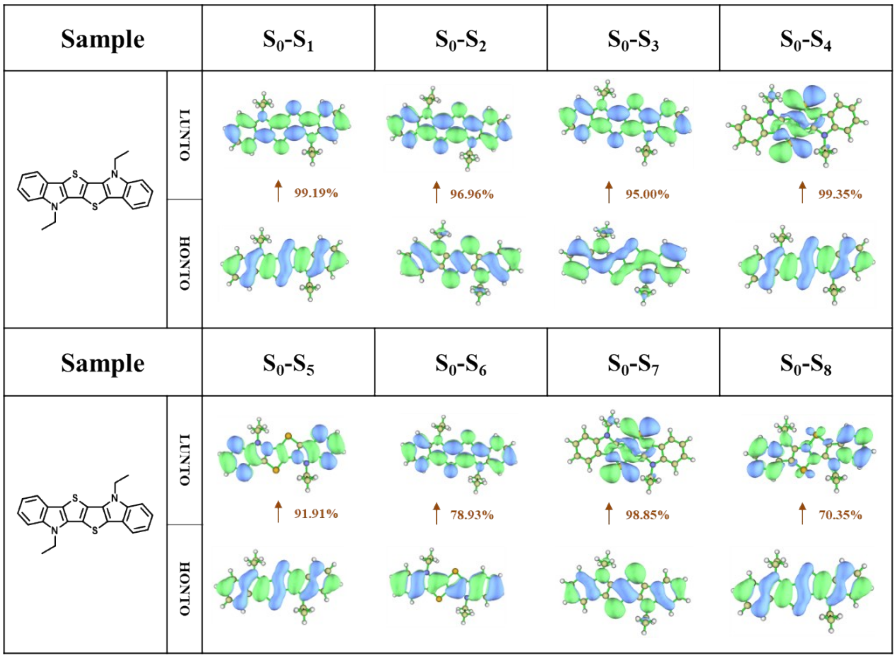

Fig.S2 HONTO and LUNTO orbital jumps of EH-PPTt, calculated by NTO(TDDFT-B3LYP/6-31G**)

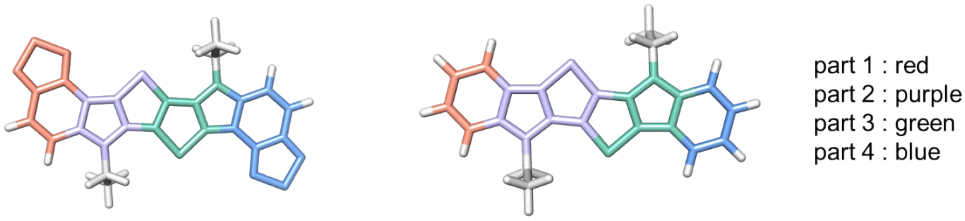

Fig. S3 The calculated results for S0→S1 from hole-electron analysis of BzPTT and EH-PPTt by TD-DFT.

Table S1 The calculated results for S0→S1 from hole-electron analysis of BzPTT and EH-PPTt by TD-DFT.

Sample	part	% hole[a]	% electron[b]	% overlap[c]	%CT[d]
BzPTT	1	13.52	40.67	23.45	27.15
	2	43.78	10.55	21.49	-33.23
	3	29.05	7.36	14.62	-21.69
	4	13.52	40.69	23.45	27.18
EH-PPTt	1	12.78	18.53	15.39	5.75
	2	41.64	41.73	41.69	0.09
	3	32.26	20.59	25.77	-11.66
	4	12.78	18.52	15.39	5.75

[a]Contribution percentage of molecule to the hole distribution of hole-electron analysis.

[b]Contribution percentage of molecule to the electron distribution of hole-electron analysis.

[c]Hole-electron overlap percentage of hole-electron analysis.

[d]Contribution percentage of the CT characteristic for S_1 states.

4. Physiochemical characteristics

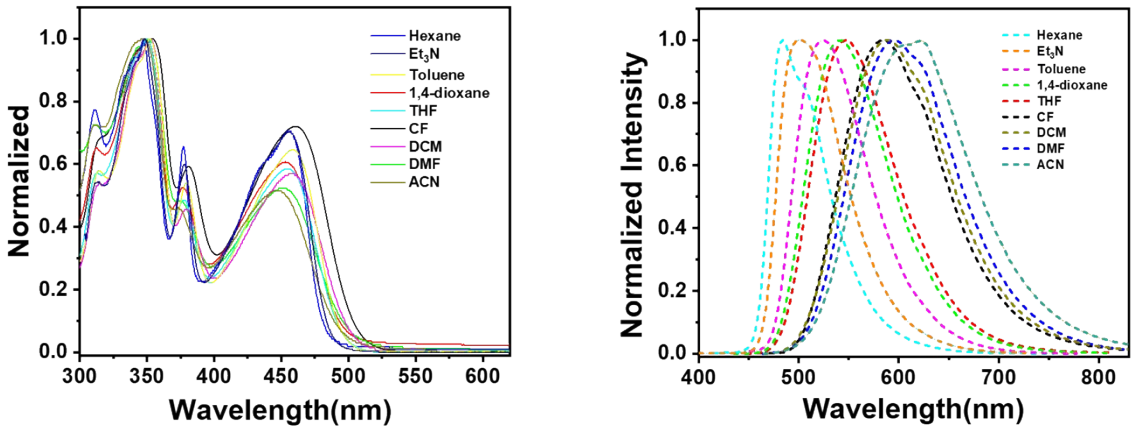

Fig. S4 UV spectra and solvatochromic effect of BzPTT C2C6 with different polarity; (THF = tetrahydrofuran; CF=chloroform; DMF = N, N-dimethylformamide; ACN= acetonitrile; DCM=dicholoromethane). [5]

Table S2 Absorption and emission peaks of BzPTT-C2C6 in different solvents. [6]

Solvent	n	ε	f (ε, n)	λ_{abs}(nm)	λ_{em}(nm)	Δν(cm^{-1})
Hexane	1.375	1.90	0.0012	457	484	1221
Toluene	1.494	2.38	0.014	458	524	2750
Et_3N	1.401	2.42	0.048	456	500	1930
1,4-dioxane	1.422	4	0.131	453	541	3591
CF	1.446	5.2	0.15	461	583	4539
THF	1.405	7.58	0.21	457	547	3600
DCM	1.424	8.93	0.217	457	590	4933
DMF	1.430	36.7	0.275	454	596	5248
ACN	1.344	37.5	0.305	447	622	6294

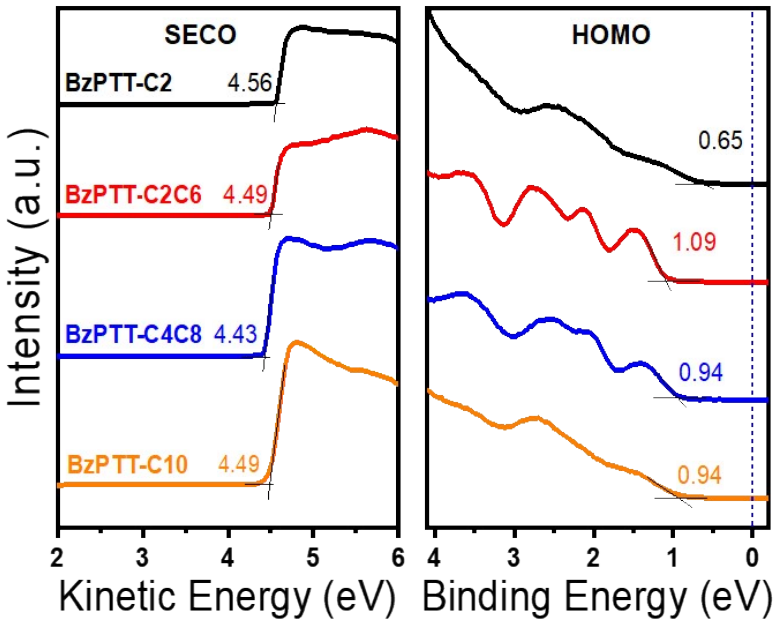

Fig. S5 UPS spectra of BzPTT-Cn films.

5. Organic Field-Effect Transistors Characteristics

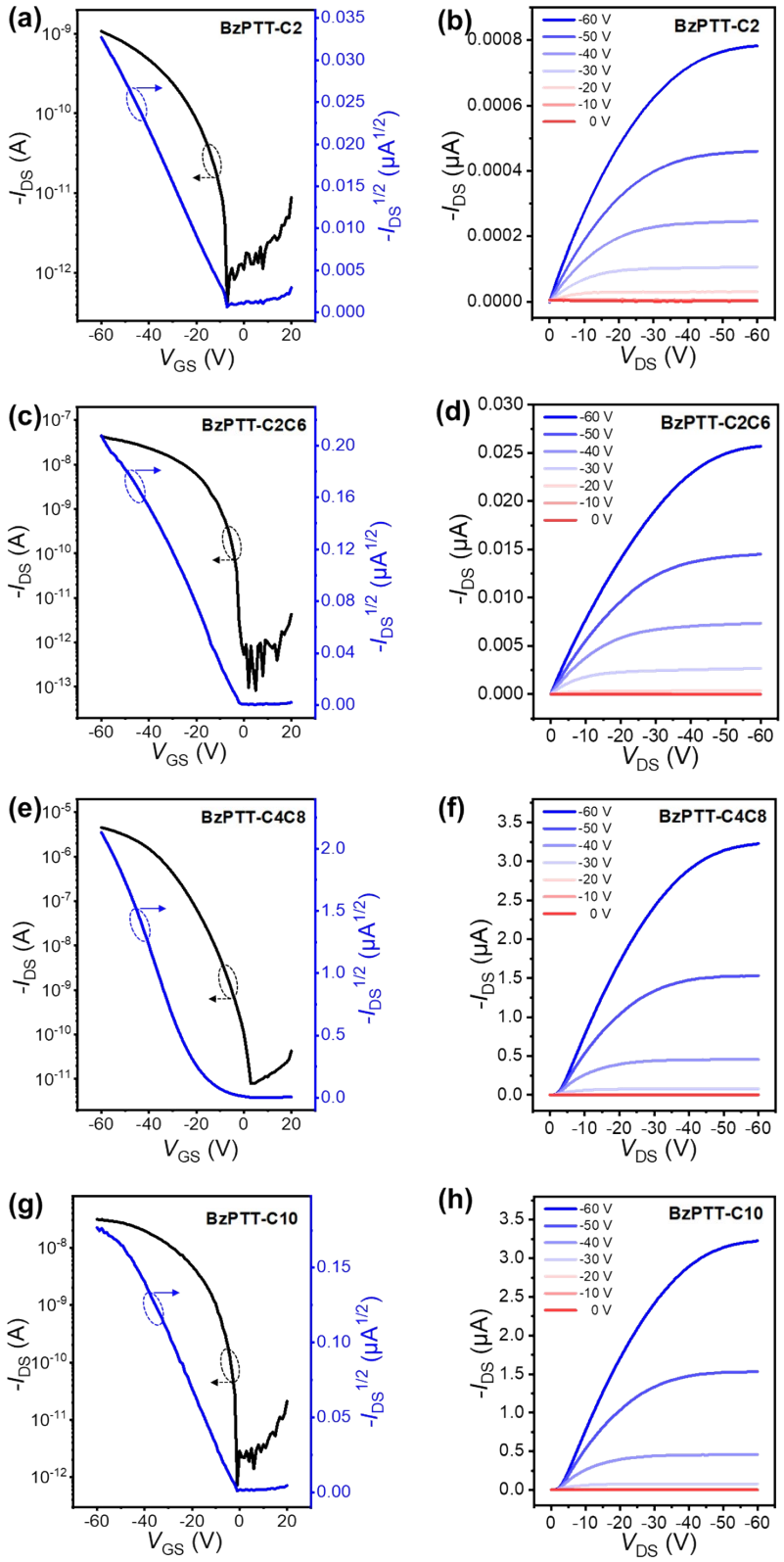

Fig. S6 The transfer (a, c, e, g) and output (b, d, f, h) curves of OFETs devices based on

BzPTT-Cn by vacuum evaporation with substrate temperature at 60 °C.

Table S3 OFETs device performance data of BzPTT-Cn with annealing substrates.

Sample	$\mu_{h,\ sat}$ [$cm^2\ V^{-1}\ s^{-1}$]	$\mu_{v,\ sat} \pm \sigma$ [$cm^2\ V^{-1}\ s^{-1}$]	V_T [V]	I_{on}/I_{off}
BzPTT-C2	1.3×10^{-4} [a], 3.4×10^{-5} [b]	$1.13 \times 10^{-4} \pm 1.22 \times 10^{-5}$ [a], $2.45 \times 10^{-5} \pm 5.90 \times 10^{-6}$ [b]	-0.3—0.3 [a], -7.9—-6.1 [b]	10^4 [a], 10^3 [b]
BzPTT-C2C6	6.0×10^{-4} [a], 9.3×10^{-4} [b]	$5.51 \times 10^{-4} \pm 6.95 \times 10^{-5}$ [a], $6.97 \times 10^{-4} \pm 2.06 \times 10^{-4}$ [b]	-11.1—-9.3 [a], -9.7—-5.7 [b]	10^5 [a], 10^4—10^5 [b]
BzPTT-C4C8	0.12 [a], 0.096 [b]	0.093 ± 0.012[a], 0.088 ± 0.012[b]	-20.6—-15.4 [a], -19.4—-17.3 [b]	10^7 [a], 10^7 [b]
BzPTT-C10	1.6×10^{-3} [a], 4.8×10^{-4} [b]	$1.35 \times 10^{-3} \pm 1.52 \times 10^{-4}$ [a], $4.20 \times 10^{-4} \pm 3.51 \times 10^{-5}$ [b]	-7.8—-6.2 [a], -3.9—-3.5 [b]	10^5 [a], 10^4—10^5 [b]
Micro-nanocrystalline of BzPTT-C4C8	0.24	0.19 ± 0.03	-11.7—-6.4	10^6

[a,] Substrate temperature of 25 °C；[b,] Substrate temperature of 60 °C.

6. Thin film morphology analysis

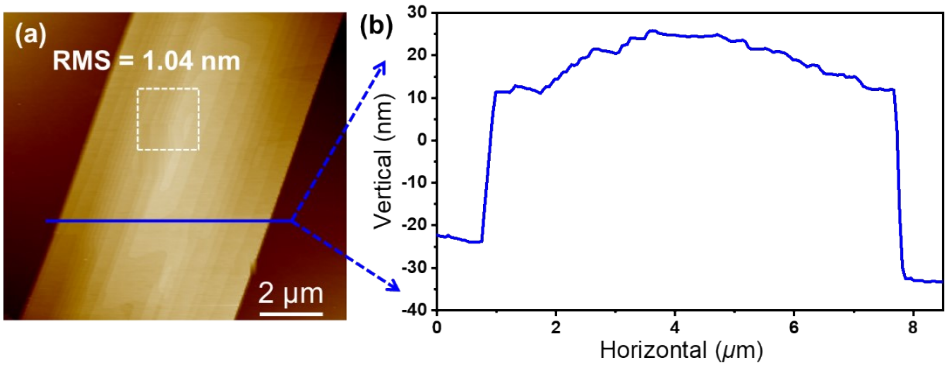

Fig. S7 AFM image (a) of BzPTT-C4C8 micro-nanocrystals prepared by PVT and heights (b) along the blue line in the image (a).

7. Organic Phototransistors Characteristics

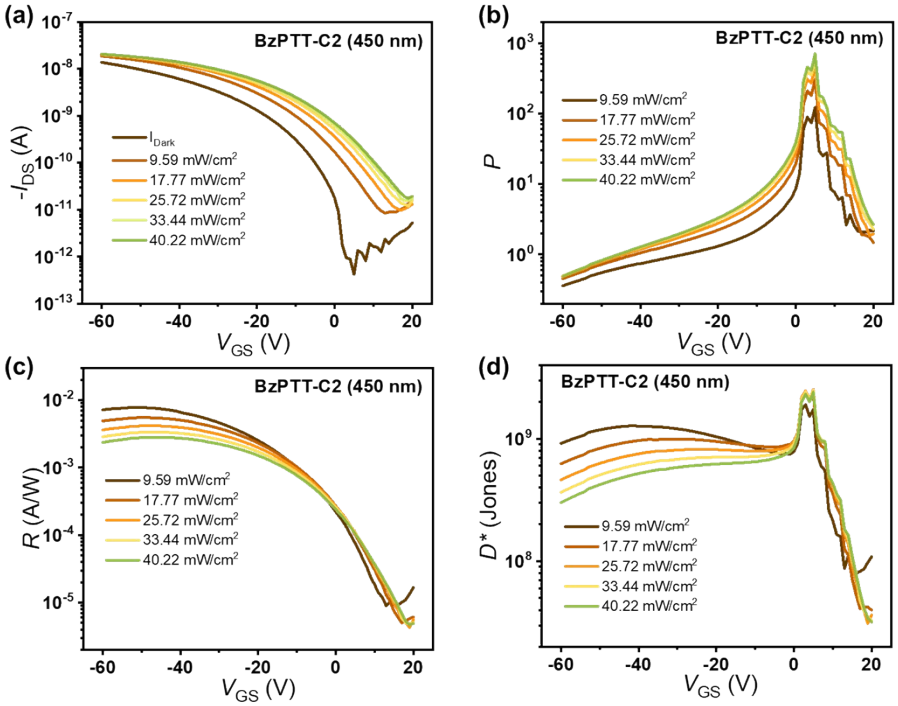

Fig. S8 Transfer (a), P (b), R (c) and D* (d) curves of BzPTT-C2-based phototransistor measured under different illumination intensities.

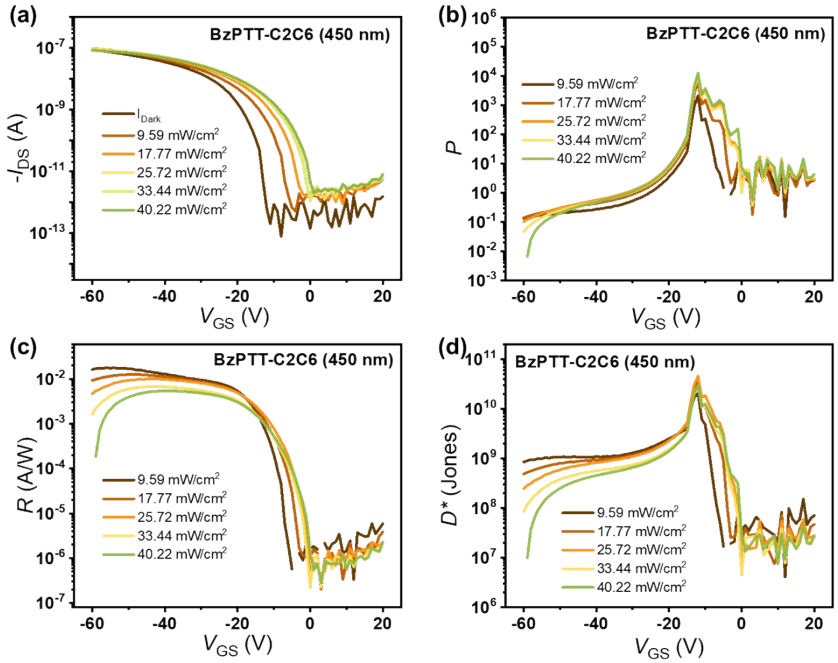

Fig. S9 Transfer (a), P (b), R (c) and D* (d) curves of BzPTT-C2C6-based phototransistor measured under different illumination intensities.

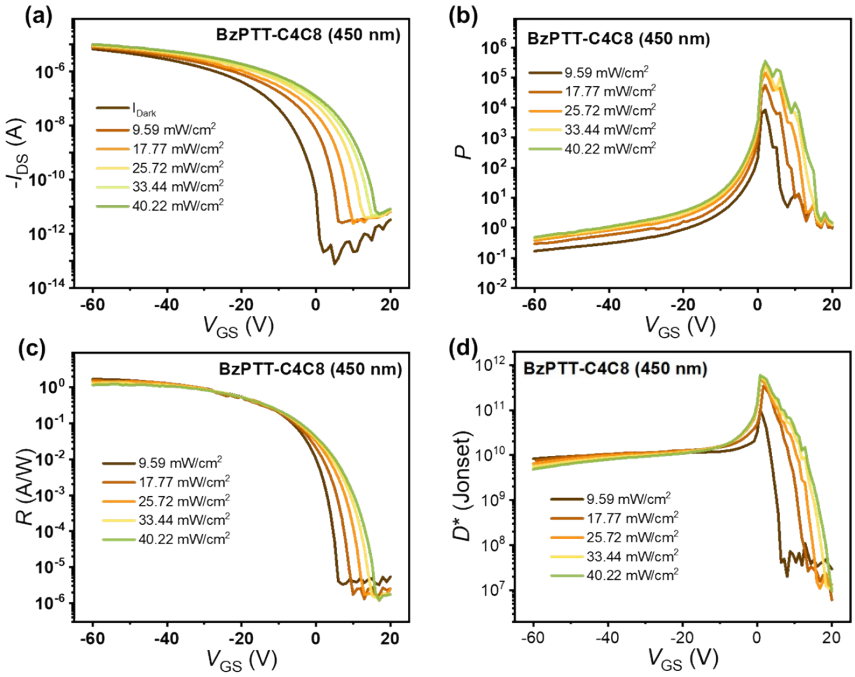

Fig. S10 Transfer (a), P (b), R (c) and D* (d) curves of BzPTT-C4C8-based phototransistor measured under different illumination intensities.

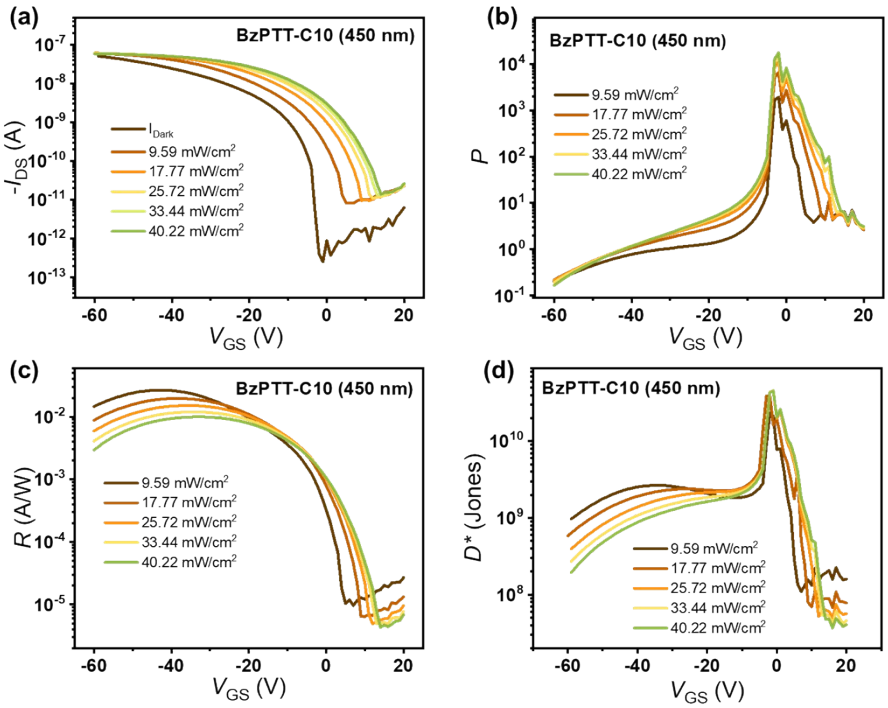

Fig. S11 Transfer (a), P (b), R (c) and D* (d) curves of BzPTT-C10-based phototransistor measured under different illumination intensities.

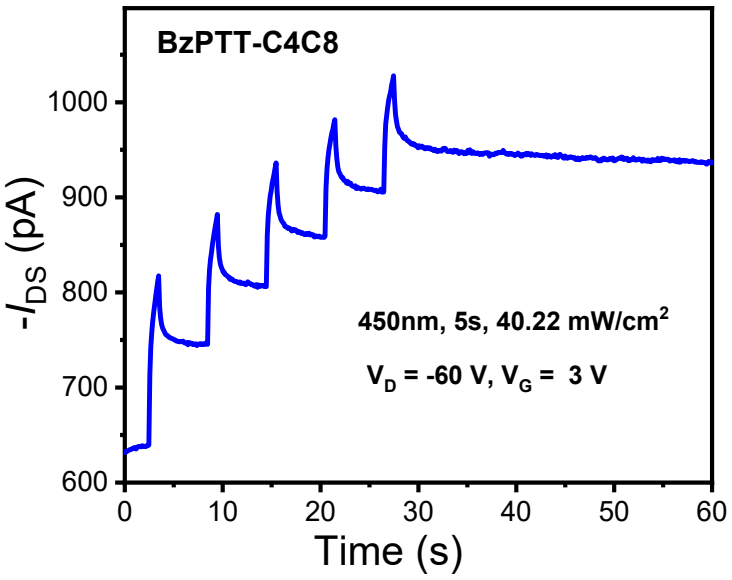

Fig. S12 Photo-switching characteristics of BzPTT-C4C8.

8. NMR and MS (MALDI-TOF) spectrum

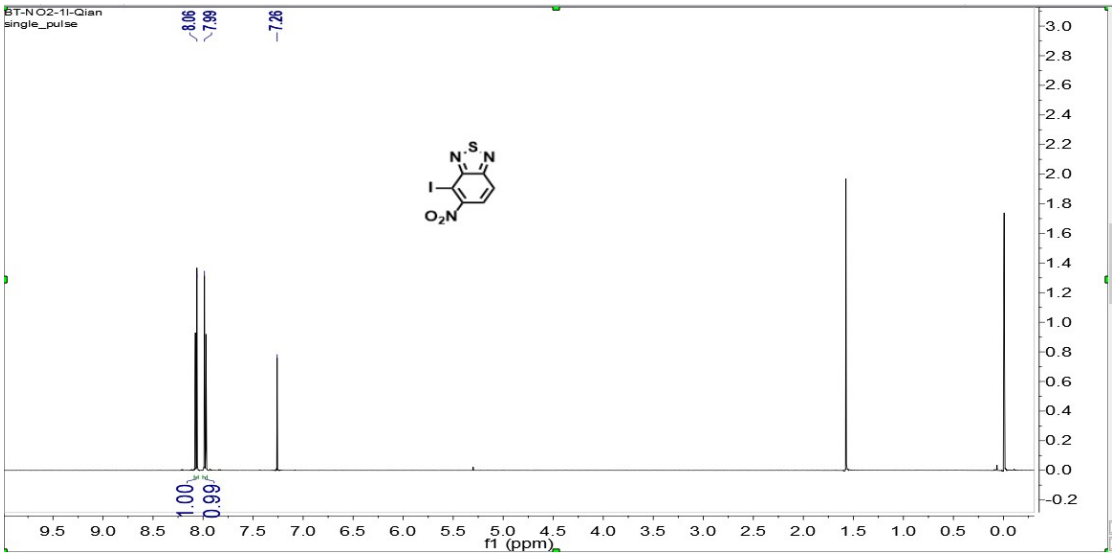

Fig. S13 ^{1}H NMR spectrum of compound 3 in $CDCl_3$ (600 MHz).

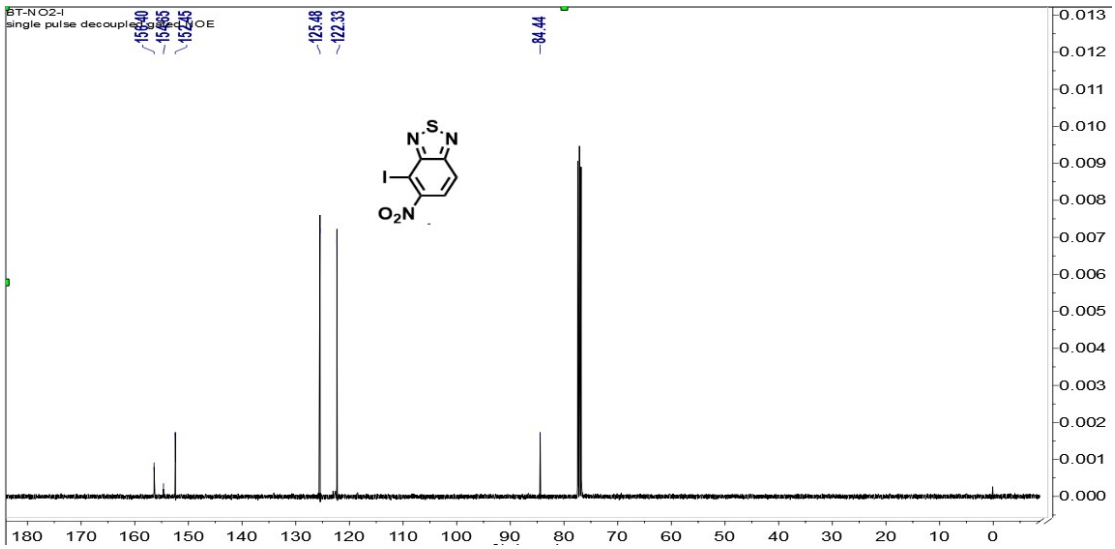

Fig. S14 ^{13}C NMR spectrum of compound 3 in $CDCl_3$ (600 MHz).

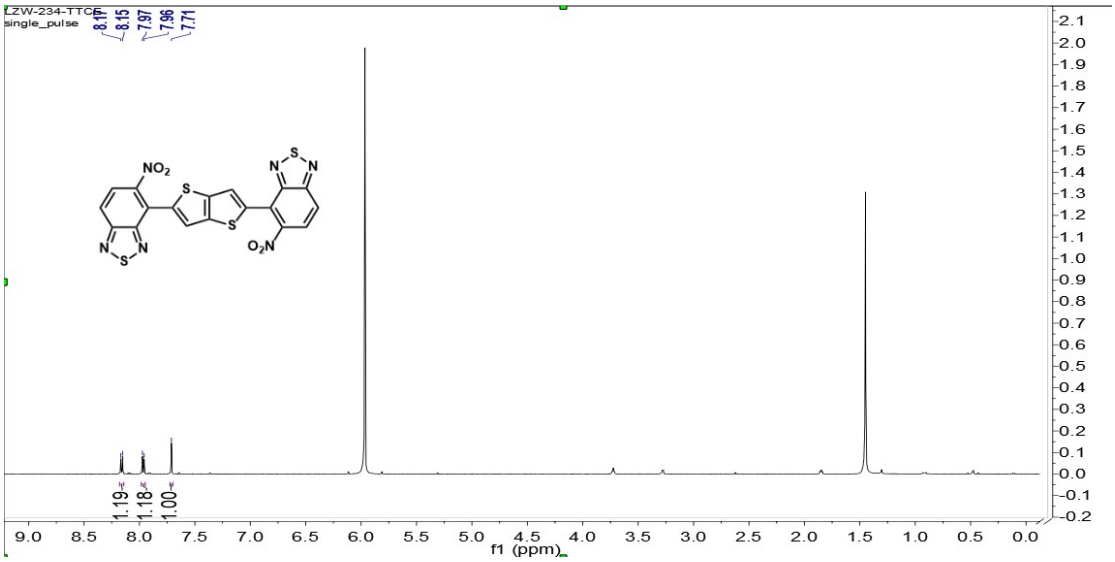

Fig. S15 ^{1}H NMR spectrum of compound 4 in 1,1,2,2-$C_2D_2Cl_4$ (100°C, 600 MHz).

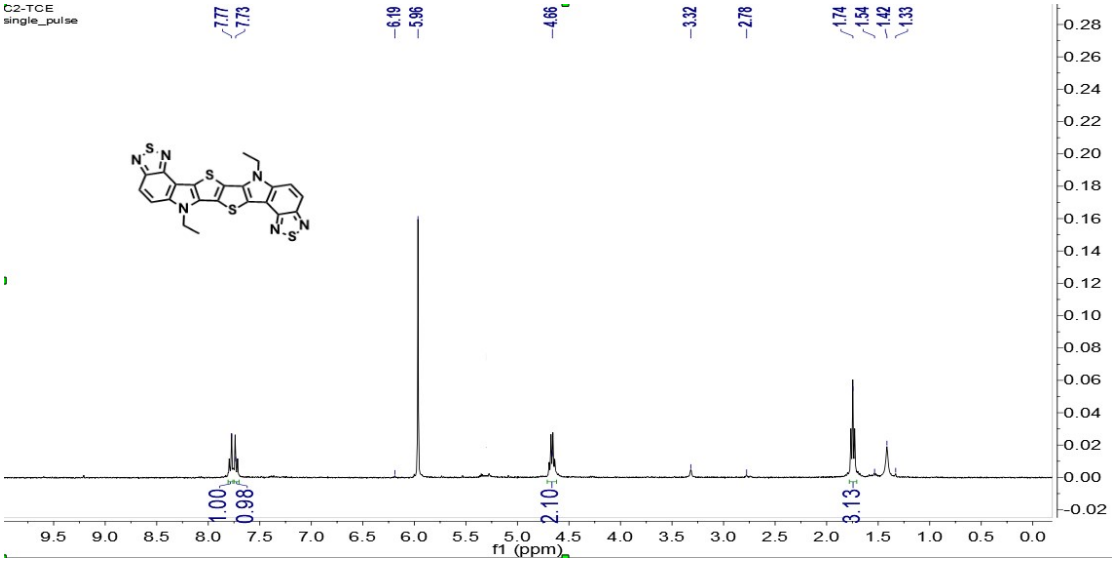

Fig. S16 ^{1}H NMR spectrum of compound BzPTT-C2 in 1,1,2,2-$C_2D_2Cl_4$ (130°C, 400 MHz).

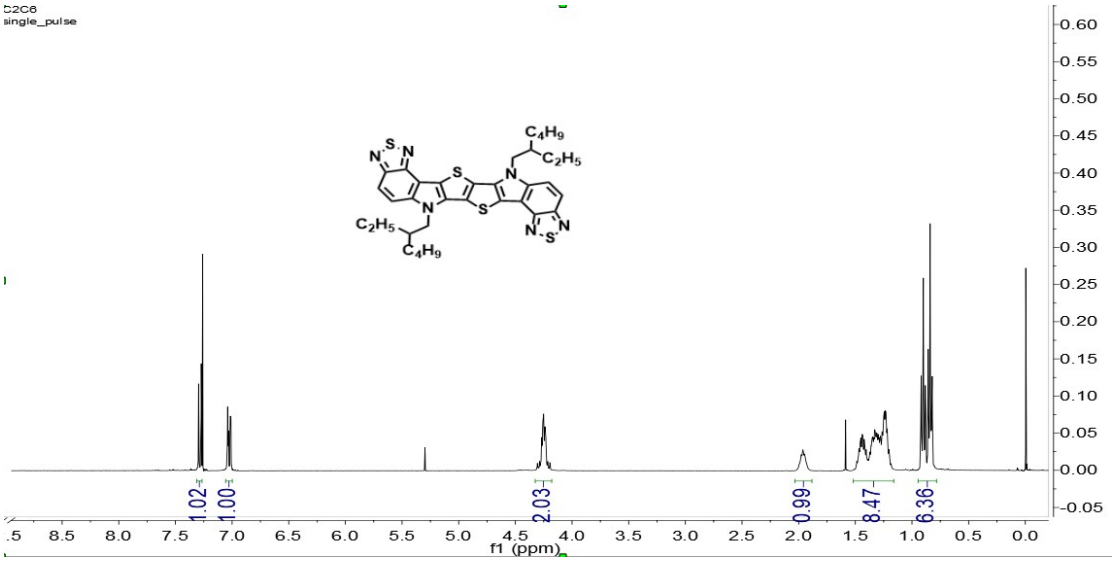

Fig. S17 ^{1}H NMR spectrum of compound BzPTT-C2C6 in $CDCl_3$ (400 MHz).

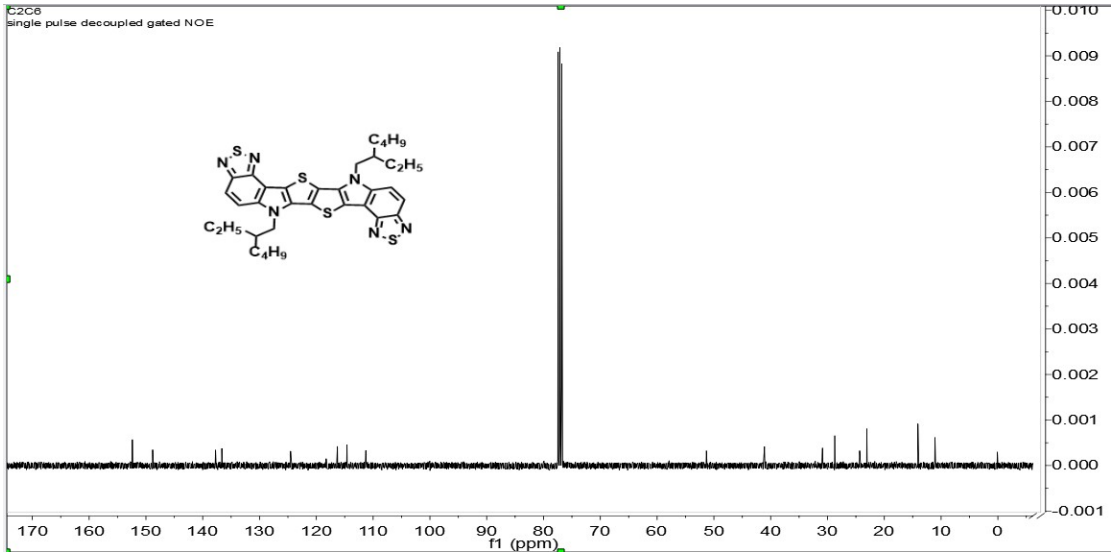

Fig. S18 ^{13}C NMR spectrum of compound BzPTT-C2C6 in $CDCl_3$ (150 MHz).

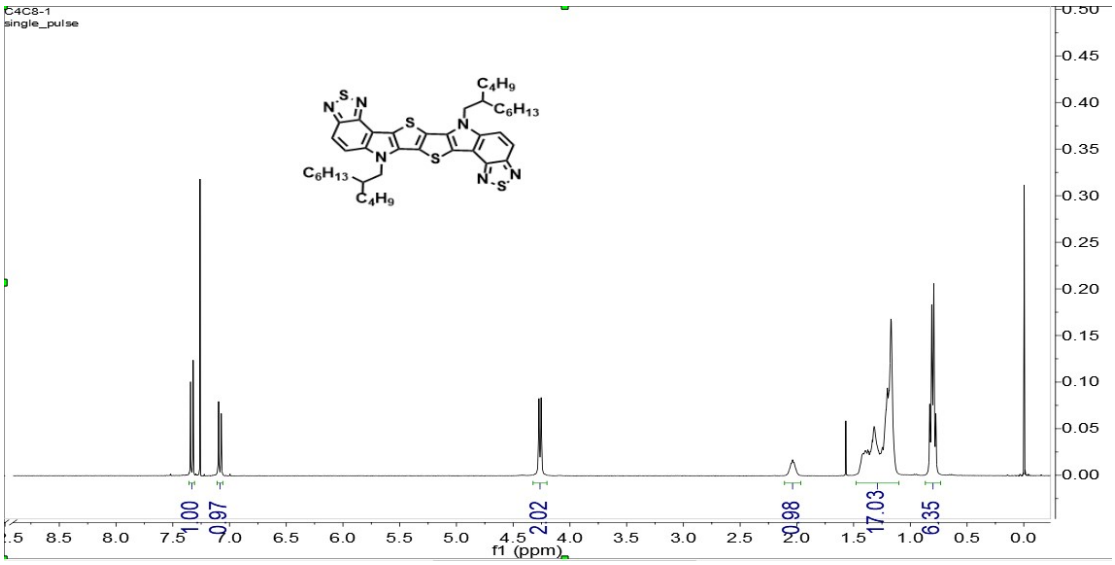

Fig. S19 ^{1}H NMR spectrum of compound BzPTT-C4C8 in $CDCl_3$ (400 MHz).

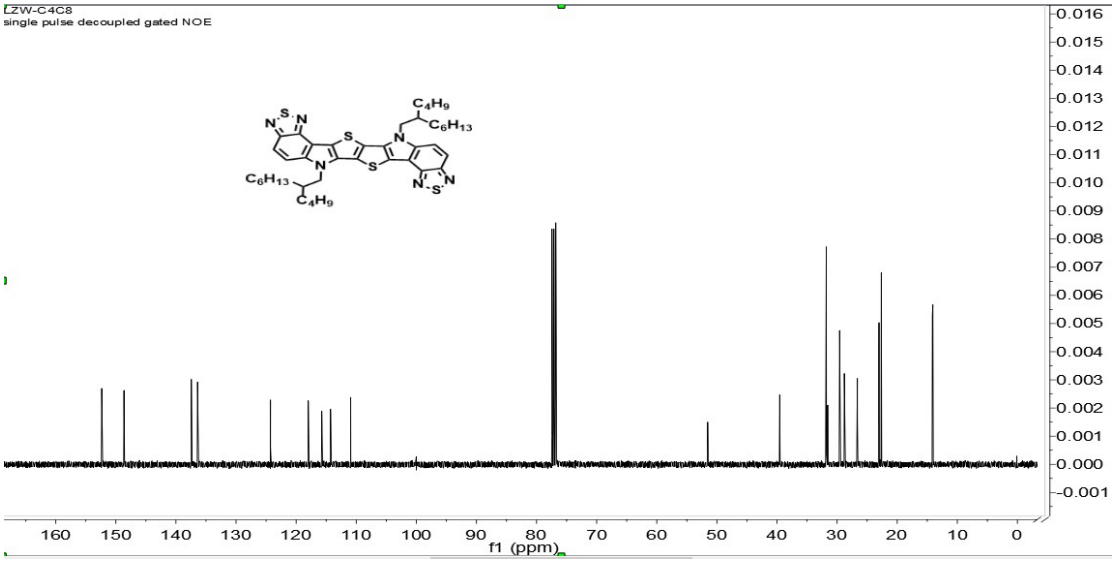

Fig. S20 ^{13}C NMR spectrum of compound BzPTT-C4C8 in $CDCl_3$ (150 MHz).

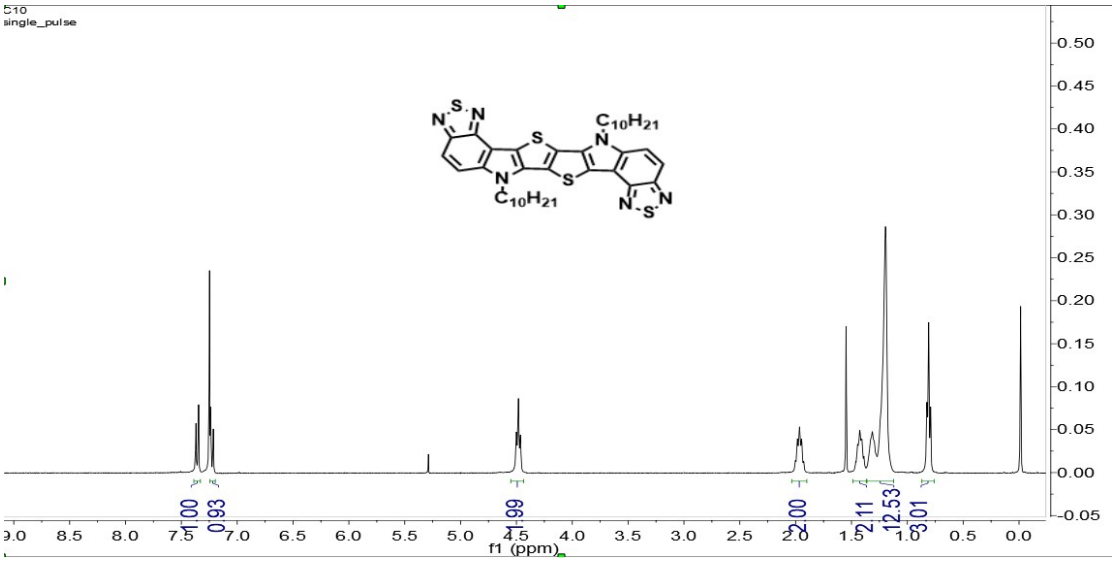

Fig. S21 ^{1}H NMR spectrum of compound BzPTT-C10 in $CDCl_3$ (400 MHz).

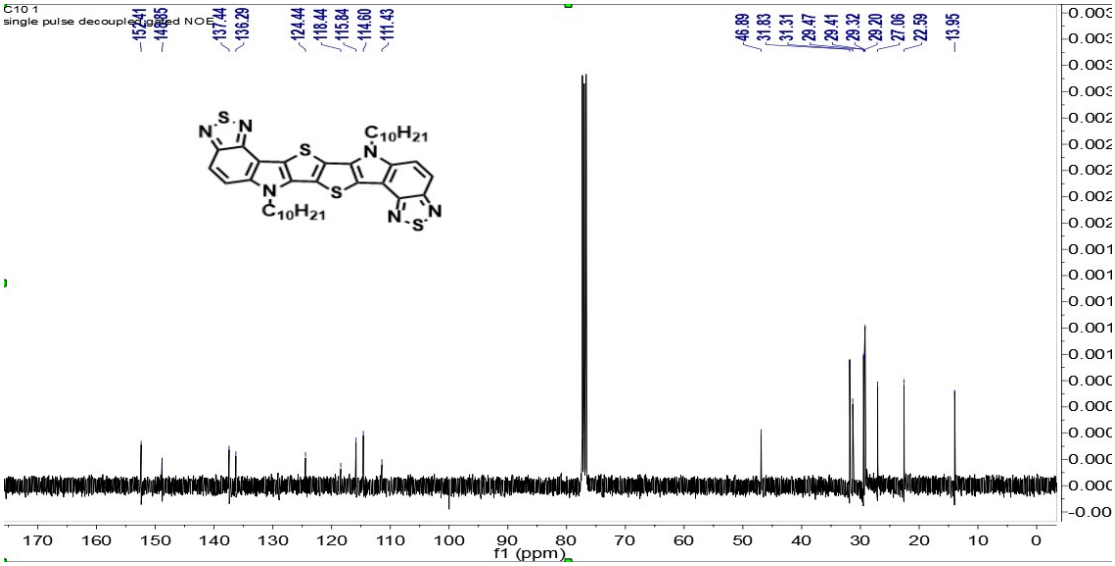

Fig. S22 ^{13}C NMR spectrum of compound BzPTT-C10 in $CDCl_3$ (150 MHz).

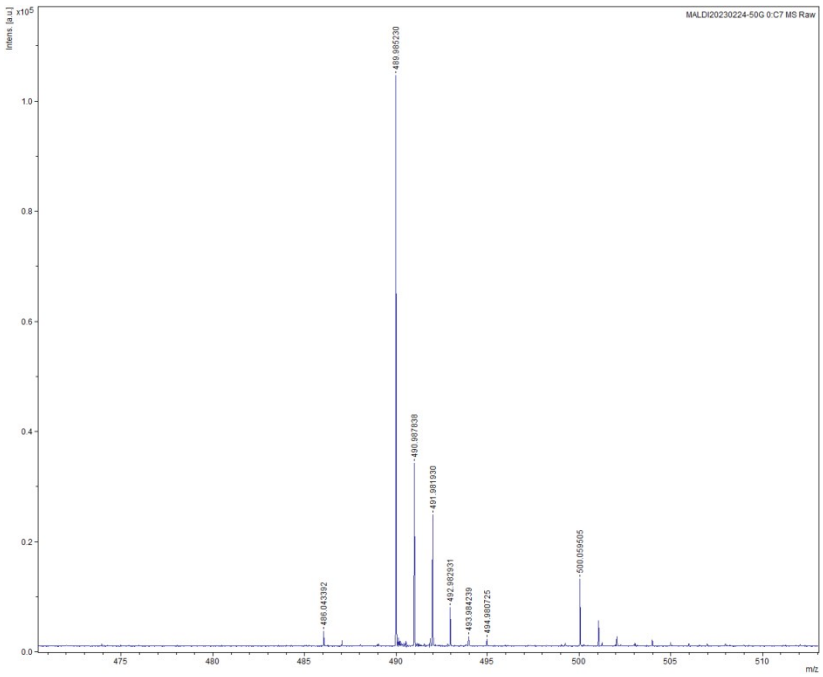

Fig. S23 MS (MALDI-TOF) spectrum of BzPTT-C2.

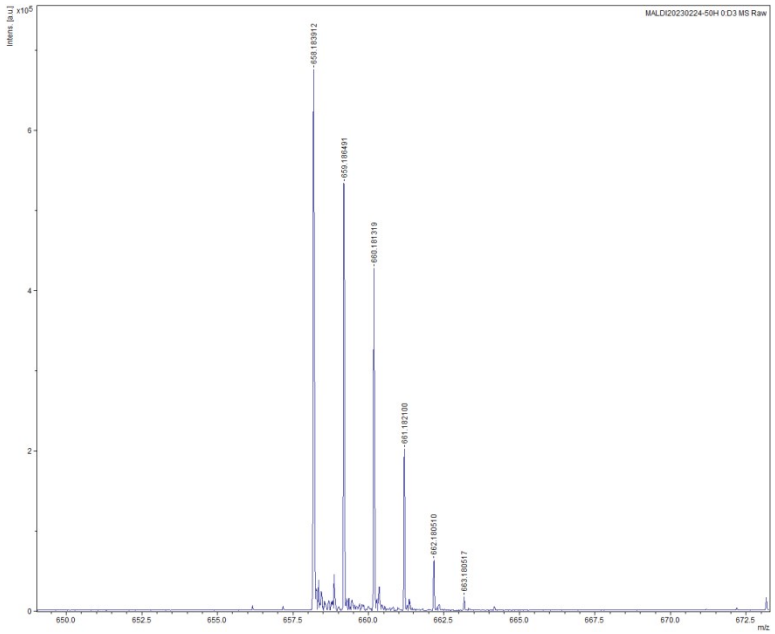

Fig. S24 MS (MALDI-TOF) spectrum of BzPTT-C2C6.

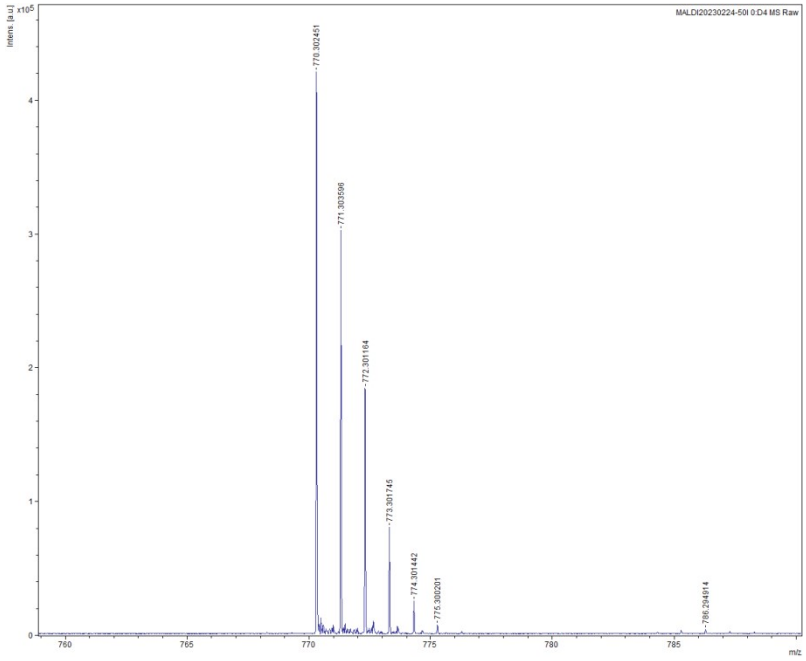

Fig. S25 MS (MALDI-TOF) spectrum of BzPTT-C4C8.

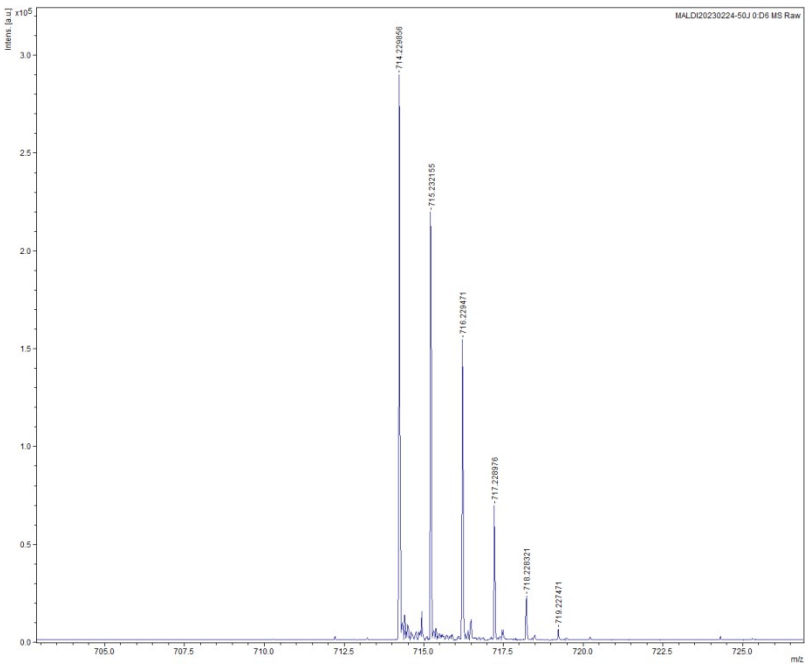

Fig. S26 MS (MALDI-TOF) spectrum of BzPTT-C10.

9. Notes and references

1 Frisch, M. J.; Trucks, G. W.; Schlegel, H. B.; Scuseria, G. E.; Robb, M. A.; Cheeseman, J. R.; Scalmani, G.; Barone, V.; Petersson; G. A.; Nakatsuji, H.; et al. Gaussian 16 Rev. A.03; *Gaussian, Inc.: Wallingford CT*, 2016.

2 LU, Tian and CHEN, Feiwu. *J. Comput. Chem.* 2012, **33,** 580–592.

3 Humphrey, W.; Dalke, A. and Schulten, K. *J. Mol. Graph.* 1996, **14**, 33–38.

4 Liu, Z., Lu, T. and Chen, Q. *Carbon*, 2020, **165**, 461-467.

5 Zhu, J., Wang, T., An, D., Zhang, R., Gu, Y., Zhou, G. and Liu, Y. *J. Am. Chem. Soc.* 2024, **146**, 21922–21931.

6 Li, W., Pan, Y., **ao, R., Peng, Q., Zhang, S., Ma, D. and Ma, Y. *Adv. Funct. Mater.* ,2014, **24**, 1609-1614.